Available online at www.sciencedirect.com
ScienceDirect
Fuel 87 (2008) 2082–2089
FUEL
www.fuelfirst.com

A stochastic simulation for the collection process of fly ashes in single-stage electrostatic precipitators

Haibo Zhao *, Chuguang Zheng

State Key Laboratory of Coal Combustion, Huazhong University of Science and Technology, Wuhan, 430074 Hubei, People's Republic of China

Received 9 May 2007; received in revised form 23 November 2007; accepted 27 November 2007
Available online 26 December 2007

Abstract

The dynamic evolution of particle size distribution (PSD) along the longitudinal length of electrostatic precipitator (ESP) quantitatively describes the collection process of ESP, and then is capable of estimating the performance of ESP. The details of the evolution of PSD are obtained by the solutions of population balance equation (PBE) for electrostatic collection. The paper promoted a stochastic method to solve the PBE. The method is based on event-driven technique and introduces the concept of weighted fictitious particles. The halving procedure of number weight of fictitious particle is adopted to restore the statistical samples of the stochastic approach and maintain the computational domain. The method, which is named event-driven constant volume (EDCV) method, is used to simulate the collection process of particles in a small-scale single-stage wire-plate ESP, considering simultaneously the electrostatic force, the convection force and the transverse particle diffusion in the model of collection kernel. The agreement among the results of the Monte Carlo method, the experimental data and the results of method of moments is good.

Keywords: Electrostatic precipitator; Monte Carlo method; Collection efficiency; Population balances; Particle dynamics

1. Introduction

Electrostatic precipitator (ESP) is a particulate control device in modern pulverized-coal-fired power plant and cement industry to collect fly ashes from a flue gas. Fly ash emissions are charged in an ESP and then are driven toward the collecting plate under the influence of an applied electrostatic field (Coulomb attraction). Compared with a mechanical ash separator such as gravitational settling and cyclone, an ESP achieves high overall mass collection efficiency, commonly above 99%. However, it is difficult for submicron particles to be collected so that amounts of toxic substances (trace metals, PAHs, etc.) in fine fly ash particles are emitted. For example, the mass collection efficiency of $PM_{2.5}$ is about 90.6% for a typical wire-plate ESP installed at a 410 t/h pulverized-coal-fired boiler [1]. Because those fine particles have a notorious impact on human health, the standards to regulate fine particle emissions are on track. To meet the new standard of pollution emissions in thermal power plant, it is necessary to reconstruct ESPs or to develop new ESPs with higher performance. The quantitative description on the collection process of fly ashes in ESPs is required for optimal design or operation.

Grade collection efficiency is usually used to evaluate the performance of an ESP. There have been numerous theoretical and experimental studies on the model of collection efficiency. Many researchers, such as Deustch [2], Cooperman [3], Leonard et al. [4], Zhao and Zhang [5], Zhang et al. [6], and Nóbrega et al. [7], had respectively conducted the models of particle collection efficiency, based on different turbulent flow field assumptions and boundary conditions. The grade collection efficiency usually considers the operation conditions (e.g., the flow velocity) and geometric structure (such as the width of wire-to-plate) of ESPs. The overall mass (or number) efficiency of polydisperse particles can be obtained through numerical integration on

* Corresponding author. Tel.: +86 27 8754 4779; fax: +86 27 8754 5526.
E-mail address: klinsmannzhb@163.com (H. Zhao).

0016-2361/$ - see front matter © 2007 Elsevier Ltd. All rights reserved.
doi:10.1016/j.fuel.2007.11.015

the grade efficiency of each size regime. However, it is impossible to obtain the details of the evolution of particle size distribution (PSD) from the model of grade collection efficiency. An understanding of the dynamic evolution of PSD must be reached for optimal configuration designs, economical operating conditions of ESPs, and the effective collection of submicron particles.

Generally, there are two kinds of numerical methods to describe the dynamic evolution of fly ashes in ESPs. One approach, in which the gas-particle turbulent model is adopted, tries to obtain the clear physical illumination of the fields through either Langrangian tracking such as direct numerical simulation (DNS) [8–10] and stochastic trajectory model [11,12], or Euler averaging such as the convective-diffusion model for particle concentration [13,14]. The complex model and the expensive cost for simulating large particle numbers constrain mostly its application. Population balance modeling (PBM), however, considers the dispersed system as a statistical ensemble, in which each dynamic event has some known probability described by some known probability functions, or saying, kernels. As far as electrostatic collection of fly ashes in an ESP is concerned, the collection kernel (or the deposition kernel) is an issue of fundamental importance. Although the occurrence of collection events of particles is involved with some complicated factors such as electrohydrodynamic (EHD) flows, turbulent flow field, particle properties and geometric parameters of an ESP, the mathematical model of the collection kernel can be obtained by theoretical and experimental studies. PBM does not try to gain the detailed information of two-phase turbulent fields and electrostatic fields, but focuses on the dynamic evolution of PSD through the solutions of population balance equation (PBE).

Though numerical methods for PBE include method of moments (MOM), sectional method, Monte Carlo (MC) method and so on, only method of moments is adopted to research the collection process of fly ashes in ESPs by Bai et al. [15] and Kim et al. [16]. The limitation of MOM lies in the demand that the initial polydispersed PSD must satisfy some special function (such as exponential distribution, lognormal distribution or gamma distribution). Then, the collection kernel must be expressed as a function of the power of particle size in order to be suitable for the moment expressions, so the Cunningham slip correction factor and the Cochet's charge equation are modified or approximated in the models of Bai et al. [15] and Kim et al. [16]. Next, MOM takes the view that the particle size distribution always satisfies the nature of "self-preserving". Last but not least, the moment equations are very complicated and are difficult to program and solve even using the familiar fourth-order Runge-Kutta method.

The paper introduces a stochastic algorithm – event-driven constant volume (EDCV) method – for the solution of PBE. The method is used to quantitatively describe the collection process of fly ashes in ESPs. The paper is organized in the following manner. In Section 2, the PBE for collection process in ESPs and the collection kernels are elaborated upon. In Section 3, the stochastic algorithm for the dynamics of the size distribution of fly ashes is introduced in details. In Section 4, numerical simulation for the collection process of fly ashes in a laboratory-scale single-stage ESP is presented. These results of the MC method are compared with the results obtained from MOM, experimental measurements and numerical solutions. The paper closes with a conclusion, which includes the discussion on the practical application of the stochastic algorithm.

2. Theoretical model

The sketch of a single-stage wire-plate ESP is shown in Fig. 1. In the most common configuration, a corona discharge is maintained in the high-voltage wire electrodes and the grounded collector plates, and molecular ions are generated near those wires. When fly ashes entrain in the flue gas flow horizontally through ducts founded by two vertical plates, the particles acquire charge by the exposure to the unipolar molecular ions that attach to each particle. The charged fly ashes migrate to the collection plates under the influence of an applied electrostatic filed. The collected fly ashes are effectively removed as large agglomerates by mechanical rapping or sonic agitation of the plate [17]. Since fly ashes are continually precipitated and do not participate in the next dynamic evolution, PSD evolves with time t, which is mathematically described by population balance equation for particle deposition (electrostatic collection) as follows:

$$\frac{\mathrm{d}n_{\mathrm{p}}(d_{\mathrm{p}},t)}{\mathrm{d}t} = -R(d_{\mathrm{p}},t)n_{\mathrm{p}}(d_{\mathrm{p}},t), \text{ or,}$$
$$\frac{\mathrm{d}n_{\mathrm{p}}(d_{\mathrm{p}},x)}{\mathrm{d}x} = -R(d_{\mathrm{p}},x)n_{\mathrm{p}}(d_{\mathrm{p}},x), \quad (1)$$

where x is the longitudinal distance from the inlet along the ESP longitudinal direction (gas flow direction); it is noted that $x = U_{\mathrm{av}}t$, t is the cumulative time from fume gas entering the ESP inlet; $n_{\mathrm{p}}(d_{\mathrm{p}}, x)$ is the size distribution function of fly ashes with diameter d_{p}, with dimension $\mu\mathrm{m}^{-1}\,\mathrm{m}^{-3}$, which means the number concentration of fly ashes with size d_{p} at distance x per unit volume; $R(d_{\mathrm{p}}, x)$ is the kernel of electrostatic collection event of fly ashes with size d_{p} at

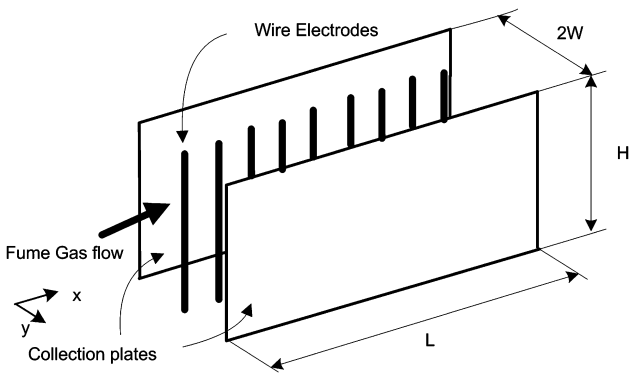

Fig. 1. Sketch of a single-stage wire-plate ESP.

distance x, meaning the collection rate of fly ashes of d_p, m^{-1}.

The model of collection kernel is one of the key issues in PBM, which depends deeply on the electric field and two-phase flows field of the collection process. Generally, the following assumptions are made for the purpose of the available mathematic model of collection kernel or collection efficiency: the collection process is considered to be steady-state; the electrostatic field is considered to be uniform, which is reasonable if space charge density is negligible; a fully developed and uniform channel flow is assumed; the gas-particle four-way coupling and the interaction between electric filed and turbulent field are neglected; non-ideal effects such as re-entrainment, the fluctuation of electric force and the pollution of discharge electrodes and collection plates are neglected; particles are spherical and its electrical resistivity is not considered; and so on.

A detailed description of the relation between collection efficiency and collection kernel is given in Appendix A. Many researchers have developed the theoretical model for collection efficiency or collection kernel based on different assumptions on the effects of turbulent mixing and "electric wind". The Deutsch model [2] assumes the complete mixing and the infinite particle diffusion transverse to the flow direction. Bai et al. [15] assumed that the transverse mixing coefficient is taken as infinity and the longitudinal mixing coefficient as zero. In fact, the finite turbulent diffusion coefficient has a significant effect on the collection process of fly ashes. Thus Cooperman [3] considered re-entrainment and finite longitudinal turbulent mixing effects; however the transverse mixing coefficient is taken as zero. The above models only describe the extreme cases, and the prediction is different from the experimental results. The model of Leonard et al. [4] is based on the finite transverse mixing coefficient and finite longitudinal mixing coefficient by solving the two-dimensional convection/diffusion equation analytically; the model [4], however, assumes the uniform turbulent dispersion coefficient and the uniform flow field, so the model cannot describe perfectly the particle diffusion process near to the collection plate. Therefore, the model of Kim et al. [16], which is based on the finite turbulent mixing effect, considered that longitudinal turbulent mixing is dominated by gas velocity, but that the particle diffusion process near the plate due to migration velocity is described by the transverse turbulent mixing. On the other side, "electric wind" or "corona wind" disturbs the flow fields near the plates, and then increases significantly the turbulence intensity [19,20]. The above models do not take the "wind" effect into account. The non-uniform air velocity profile and the effect of turbulent mixing by "electric wind" are considered by Zhao and Zhang [5]. Nevertheless, the above models used an improper boundary condition at the central plane. A zero flux boundary condition at the center plane is adopted by Zhang et al. [6] and Nóbrega et al. [7], respectively, based on the former model of Leonard et al. and the former model of Zhao and Zhang.

Different models of collection efficiency show different performances on different cases. As for a laboratory-scale ESP that is described in literature [19], the model of Zhao and Zhang [5] is found to be in a better agreement with the experimental data than the models of Deutsch [2], Cooperman [3] and Leonard et al. [4]. As far as the experimental setup of Nóbrega et al. [7] is considered, the model of Nóbrega et al. [7] shows higher precision than the model of Zhao and Zhang [5]. With respect to the experimental ESP of Salcedo and Munz [21], the results predicted by the models of Zhang et al. [6] and Kim et al. [16] agree better with the measured overall mass efficiency. In the paper, the collection kernel of Kim et al. [16] is adopted because of its precision and its simplified representation as following:

$$R(d_p) = \frac{\omega^2}{2U_{av}D_2}, \tag{2}$$

where U_{av} is the average longitudinal flow velocity, m s^{-1}; ω the particle migration velocity; D_2 the particle transverse diffusion coefficient; $D_2 = D_B + D_t$; D_B the Brownian diffusivity; D_t is the turbulent diffusivity. Those parameters are calculated as follows [22,23]:

$$\omega = \frac{qE_cC_c}{3\pi\mu d_p}; \quad q = \pi\varepsilon_0 E d_p^2\left[\left(1+\frac{2\lambda_i}{d_p}\right)^2 + \frac{2}{1+2\lambda_i/d_p}\frac{\kappa-1}{\kappa+2}\right];$$
$$C_c = 1 + 2.493\frac{\lambda}{d_p} + 0.84\frac{\lambda}{d_p}\exp\left(-0.435\frac{d_p}{\lambda}\right);$$
$$D_B = \frac{k_BTC_c}{3\pi\mu d_p}; \quad D_t = 0.12U_\tau W;$$
$$U_\tau = \sqrt{\frac{fU_{av}^2}{8}}; \quad f^{1/2} = -\frac{1}{1.8\lg(6.9/Re)}; \quad Re = \frac{2\rho U_{av}W}{\mu}, \tag{3}$$

where q is the particle charge; C_c the Cunningham slip correction factor; E_c the electric field strength at the collecting plate surface; E the local electric field strength of the charge; in the paper it is considered that $E_c = E$; μ the gas viscosity; ε_0 the permittivity of free space ($=8.85\times10^{-12}$ F m^{-1}); λ the gas mean free path; λ_i the ionic mean free path; κ the dielectric constant of particles; k_B the Boltzmann constant ($=1.38054\times10^{-23}$); T the gas absolute temperature, K; W the width of wire-to-plate; U_τ the friction velocity; f the friction factor; Re the Reynolds number of fume gas flow; ρ the gas density.

According to Eq. (A-3), the grade number collection efficiency is numerically calculated by

$$\eta_n(d_p, x) = 1 - \exp\left[-\frac{\omega^2 x}{2U_{av}D_2}\right]. \tag{4}$$

3. The introduction of event-driven constant volume method

The authors have developed the so-called multi-Monte Carlo (MMC) method to describe the time evolution of particle size distribution, and MMC method is used to

consider the dry deposition of particles in a closed chamber [24] and wet removal of aerosol by precipitation [25]. The MMC method introduces the concept of "weighted fictitious particle" and is based on the "time-driven" MC technique. The number weigh of the involved fictitious particles is continually adjusted so as to forcibly maintain both the total number of fictitious particles and the computational domain. However, the original MMC method exhibits so-called "uncoupling error" [26], which originates from the uncoupling process of dynamic events within one time step in "time-driven" MC technique. Furthermore, the method performs so-called "constant volume error" [26], owing to the forcible maintenance of particle number and computational domain, which disturbs the number weight of fictitious particle. The paper demonstrates a new event-driven constant volume (EDCV) method for electrostatic collection event.

The EDCV method still introduces the concept of "weighted fictitious particle" [27], saying, those real particles that have the same or similar size are represented by one or several weighted fictitious particles. The dynamic evolution of fictitious particles duplicates that of real particles. The weighted fictitious particles are generated according to the following steps: bin discretization of real particle population is taken firstly, and then every bin is represented by some fictitious particles. The value of number weight "w_p" of one fictitious particle is equal to the number of those real particles represented by the fictitious particle. The total number of fictitious particles is much less than that of real particles. The EDCV method tracks the dynamic evolution of fictitious particle population. These fictitious particles of the same bin have the same value of number weight "w_p", however the different values for different bins. Those measures assure that the fictitious particles population duplicates the statistical information of real particle population as much as possible.

Different from the MMC method, the EDCV method is founded on the framework of the "event-driven" MC technique, which describes the collection process in three steps. Firstly, the interval of quiescence of two events Δt is calculated as following:

$$\Delta t_k = 1/(V_s E_{depo}) = 1\Big/\left(V_s \int_{d_p} R(d_p) n_p(d_p) \mathrm{d}d_p\right) = 1\Big/\sum_{i=1}^{N_f} R_i, \tag{5}$$

where V_s is the real-time volume of computational domain, E_{depo} is the real-time electrostatic collection rate per unit volume ($m^{-1}\,m^{-3}$), N_f is the total number of fictitious particles, R_i is the collection kernel of particle indexed by i.

Secondly, the main particle, i.e., the particle that is collected by ESPs after the interval of quiescence Δt, is selected by the cumulative probabilities method [28] according to the following relation:

$$\sum_{m=1}^{i-1} R_m \Delta t < r \leqslant \sum_{m=1}^{i} R_m \Delta t, \tag{6}$$

where r is a random number from a uniform distribution in the interval [0,1]. If the relation (6) is satisfied, it is considered that the fictitious particle i is the main particle.

Lastly, the consequence of the electrostatic collection event of the main particle i is treated. The EDCV method does not forcibly keep the total number of fictitious particles constant throughout the simulation process, which is different form the MMC method. The main particle i is discarded and not be tracked any longer in the simulation. So, one collection event means subtracting one from the total number of fictitious particles. Along with the dynamic evolution of dispersed system, the total number of fictitious particles will be smaller and smaller, which will deteriorate the statistical precision of MC method. Illuminated by stepwise constant volume method [29], the EDCV method adopts a so-called "stepwise constant number scheme" to restore the total number of fictitious particles. When the number of fictitious particles reaches to $N_{f,0}/2$ (where $N_{f,0}$ is the initial number of fictitious particles), the surviving particles are duplicated and added into fictitious particle array to restore the number of fictitious particles. As a result, the number weight of each fictitious particle is halved. In the next time step, the new fictitious particle population is tracked. The halving procedure of the number weight still maintains continuously the computational domain, however maintains the total number of fictitious particles step by step.

The proposed method is used to solve indirectly PBE for electrostatic collection event, and the dynamic evolution of size distribution along the longitudinal distance x is obtained.

4. Numerical simulation for the collection process of fly ashes in an ESP

4.1. Initial conditions

Usually, it is considered that the size distribution of fly ashes at the inlet of an ESP is represented by the lognormal distribution:

$$n_p(d_p) = \frac{N_p}{\sqrt{2\pi}\ln\sigma_{pg}} \exp\left[-\frac{\ln^2(d_p/d_{pg})}{2\ln^2\sigma_{pg}}\right]\frac{1}{d_p}, \tag{7}$$

where N_p, d_{pg} and σ_{pg} are the number concentration, the geometric mean size and the geometric standard deviation, respectively. A small laboratory-scale ESP measured by Salcedo and Munz [21] is considered in the simulation. The experimental conditions are summarized as following: the initial geometric mean size ($d_{pg,0}$) is 1.5 μm; the initial geometric standard deviation ($\sigma_{pg,0}$) is 1.76; the width of wire-to-plate (W) is 0.081 m; the height of plate (H) is 0.38 m; the length of ESP (L) is 2.53 m; the discharge electrodes are placed 0.152 cm apart; the radius of the corona

wire is 0.06 cm; the applied voltage (V_w) is 38 kV, the average electric field strength at the collecting plate surface ($E_c = V_w/W$) is 4.69 kV cm^{-1}; the gas density (ρ) is 0.8288 kg m^{-3}; the gas viscosity (μ) is 2.4×10^{-5} kg m^{-1} s^{-1}; the particle density (ρ_p) is 3600 kg m^{-3}; the dielectric constant of particles (κ) is 3.6; the average longitudinal flow velocities (U_{av}) are 2 ms^{-1}, 3 ms^{-1} and 5 ms^{-1} in different operation cases; $\lambda = 6.5 \times 10^{-8}$ m, $\lambda_i = 1 \times 10^{-7}$ m, $\varepsilon_0 = 8.85 \times 10^{-12}$ F m^{-1}. In the simulation, the initial number concentration ($N_{p,0}$) is chosen as 10^{10} m^{-3}; the range of size distribution is considered as $\ln d_{pg,0} - 4\ln\sigma_{pg,0} \leqslant \ln d_p \leqslant \ln d_{pg,0} + 4\ln\sigma_{pg,0}$, i.e., $0.156\ \mu m \leqslant d_p \leqslant 14.393\ \mu m$. The size distribution is divided into 200 bins between the largest and smallest particle size, logarithmically spaced. Every bin is represented by 100 fictitious particles at least. The initial number of fictitious particles is 21,832 according to those procedures.

4.2. The dynamic evolution of size distribution along longitudinal ESP length

The EDCV method can obtain the details of each fictitious particle along the incremental ESP length, and then the evolution of some "macro-parameters" (for example, the number concentration, the geometric mean size, the geometric standard deviation, the overall collection efficiency, etc.) and some "micro-parameters" (for example, the grade collection efficiency, the cumulative undersize distribution, and the size distribution function, etc.) are counted according to Eqs. (A-7)–(A-13). Those parameters of particle size distribution will be helpful of the design, operation optimization and the performance evaluation of ESPs.

Fig. 2 shows the change of overall mass efficiencies at the different air velocities against incremental ESP length. The simulation results of method of moments [16], the EDCV method and the measured data by Salcedo and Munz [21] are compared in the figure. Obviously, the agreement between EDCV results and MOM results is good, and the simulation results of the two methods agree well with the experimental results on the whole. The little difference between the results of the two methods lies in that MOM [16] adopts the simplified model of the Cunningham slip correction factor and Cochet's charge equation, and omits the effect of Brownian diffusion. The good agreement between the results of the two method shows that, on the one hand, the EDCV method describes rightly the dynamic evolution of particles in the ESP; on the other hand, the simplified kernel models adopted by MOM [15,16] is reasonable in the laboratory-scale ESP.

The numerical solution of grade number collection efficiency can be obtained according to Eq. (A-3), which is comparable with the corresponding statistical results of the EDCV method. Fig. 3 presents the results of grade number collection efficiency at different SCAs for $U_{av} = 2$ m/s, where SCA ($=x/(U_{av}W)$) denotes the specific collection surface defined as the ratio of the total collection area to the total gas volume flow rate, with dimension s m^{-1}. It is obvious that the predicted results agree well with those of numerical solution. The simulation results of EDCV method fluctuate around the numerical results, which is ascribed to the inevitable statistical error of MC method.

The cumulative undersize distribution, $Y(d_p, x)$, is also one of important performance parameters in an ESP, meaning the ratio of the mass sum of particles with a diameter smaller than d_p to the total mass of particle population at x. The numerical results of $Y(d_p, x)$ are also obtained through counting the particle size distribution along the ESP length, where it is assumed that the densities of fly ashes with different sizes are the same. Because $Y(d_p, x)$ is an accumulative quantity and then the stochastic disturbance of MC method is erased, the curve of $Y(d_p, x)$ is much smoother and more regular than that of $\eta_n(d_p, x)$, as shown in Fig. 4.

The results exposed in Figs. 4 and 5 clearly show that: those particles with small size (such as $PM_{2.5}$) are difficult to be collected by the ESP; however, the ESP effectively collects fly ashes with diameter 10 μm or larger, almost

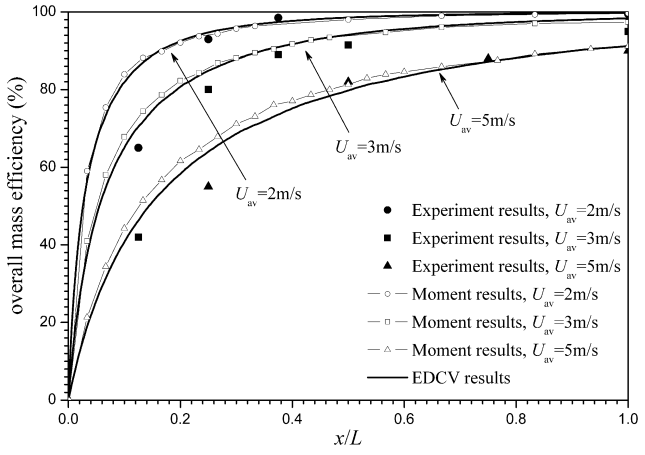

Fig. 2. The evolution of overall mass collection efficiency.

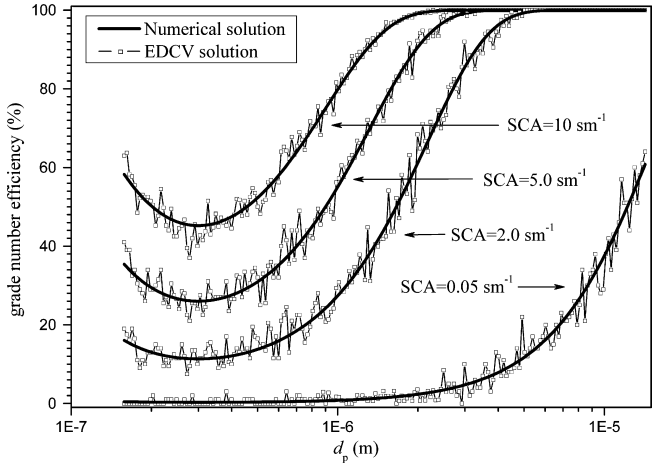

Fig. 3. Evolution of grade number collection efficiency.

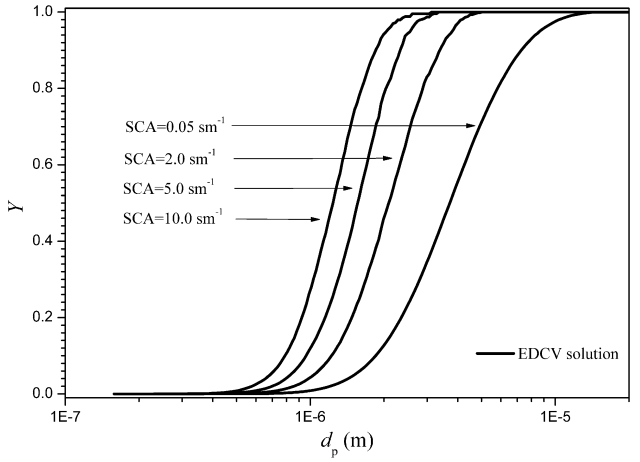

Fig. 4. Evolution of cumulative undersize distribution curve.

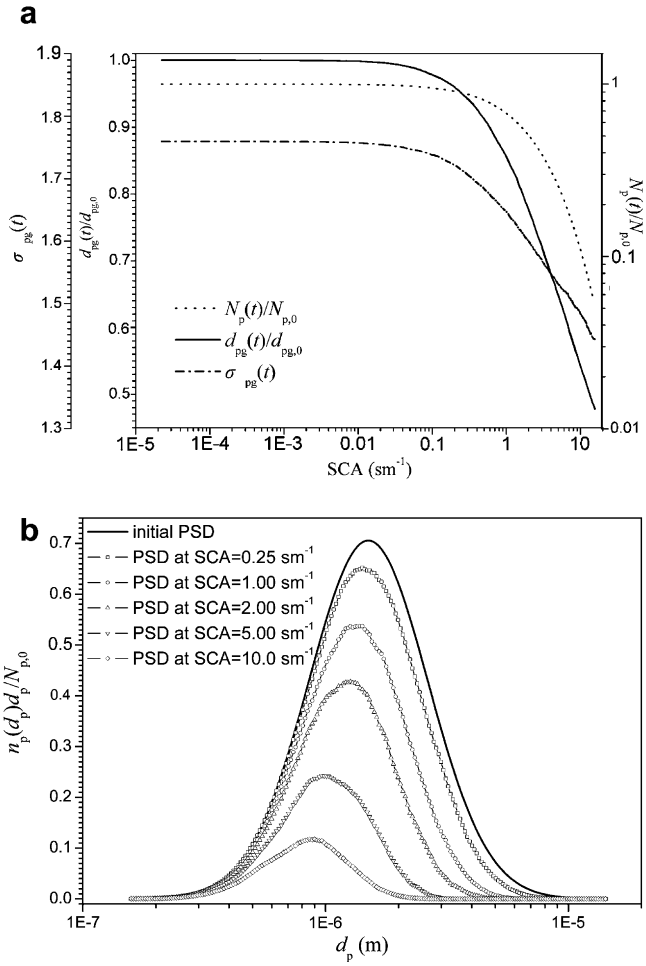

Fig. 5. Evolution of N_p, d_{pg}, σ_{pg} and particle size distribution. (a) N_p, d_{pg}, σ_{pg}; (b) particle size distribution at some special lengths.

close to 100%. For example, at SCA = 2.0 s m^{-1}, the grade collection efficiency of particles of 10 μm, η_n(10 μm, 2.0 s m^{-1}), is about 100%, and the cumulative undersize distribution of PM_{10}, Y(10 μm, 2.0 s m^{-1}), is also close to 100%; then, η_n(2.5 μm, 2.0 s m^{-1}) ≈ 75%, Y(2.5 μm, 2.0 s m^{-1}) ≈ 67%; next, η_n(0.3 μm, 2.0 s m^{-1}) ≈ 11%, Y(2.5 μm, 2.0 s m^{-1}) ≈ 0%; however, the grade number collection efficiency of 0.16 μm-particles increases slightly compared with that of 0.3 μm-particles and reaches to 16%. In conclusion, the grade number collection efficiency will first decrease next increase and then reach to 100% against the incremental particle size. The minimum of grade number collection efficiency appears at $d_p = 0.3$ μm. The semi-parabola of grade number collection efficiency is explained as the competition between the electric force and the inertia of particle. The larger size of particle results in the larger total surface area of the particle and then the more electric charge and then the larger electric force imposed on the particle, which is also exposed in Eq. (3). On the other hand, the larger size results in the bigger mass and then the bigger inertia of the particle. The two forces imposed on the particle complete each other. The inertia force dominates the collection process of the particles when particle size is smaller than 0.3 μm; then the electric force "defeats" the inertia force against the incremental particle size.

The longitudinal evolution of particle size distribution can be obtained by counting fictitious particle population at different SCAs. Fig. 5a shows several statistic macro-parameters including the specific total number ($N_p/N_{p,0}$), the specific geometric mean size ($d_{pg}/d_{pg,0}$), the geometric standard deviation along with the SCA. The evolution of PSD is plotted in Fig. 5b. As the SCA increases (the longitudinal distance x increases), the curve of particle size distribution becomes lower and flatter, which indicates that the number concentrations of particles of any sizes become smaller and smaller, sayings, ESP collects particles with different sizes more or less. The curve of particle size distribution continues to shift to left side, which means that ESP collects large particles more effectively than small particles. As shown in Fig. 5a, the total number concentration, the particle geometric mean size and the particle geometric standard deviation decrease obviously along with ESP length.

5. Conclusions

The paper proposed a stochastic method, the event-driven constant volume (EDCV) method, to solve the population balance equation (PBE) for the electrostatic collection event in ESPs. The dynamic evolution of particle size distribution is quantitatively obtained, and then the collection process of particles by ESPs is quantitatively described. This method can obtain the dynamic evolution of not only macro-parameters (such as the total particle number, the geometric mean size, the geometric standard deviation and the overall mass efficiency) but also micro-parameters (e.g., size distribution function, the grade collection efficiency and the cumulative undersize distribution). The collection efficiency obtained by this method is in good agreement with the corresponding numerical solutions, experimental data, and the results of method of moments. Compared to method of moments, the EDCV method does not need any constraints on the initial particle size

distribution, and any assumptions or simplifications on the collection kernel.

However, it is worth noting that the collection process of particles in ESPs is very complex. The model of collection kernel in the paper did not consider the non-uniformity and fluctuation of gas flow field and the electrostatic field, as well as the interaction among the particle field, the gas flow field and the electrostatic field. The boundary conditions and the temperature field are also be simplified. Some geometrical structure (for example, the wire-to-wire spacing, the diameter of discharge wire, etc.) and operation types (such as the types of rapping system, re-entrainment) of ESPs are not considered in the kernel model. Some abnormal cases of electrodes and collection plates, such as the pollution of electrodes, are not included in the kernel model. The predictions of the collection kernel in the paper are limited to the ESPs under the condition of low electro- and hydrodynamic flow effects [16]. In order to take properly the above factors into account, more complex and exacter collection kernel must be developed from the detailed numerical simulations (such as the results of direct numerical simulation [8–10]) or the experimental results [18,19]. The prediction accuracy of the MC method is mainly determined by the collection kernel. Once the collection kernel, initial particle size distribution and operation conditions of ESPs are gained, the MC method can describe the collection process of fly ashes in ESPs quickly and exactly. The EDCV method costs about 3–5 min to finish one operation case in the paper. On the other hand, the EDCV method can be coupled with the particle trajectory model to obtain the clear profile of electrohydrodynamic flows in ESPs, in which the computation cost will be saved greatly.

Acknowledgements

The authors were supported by "National Key Basic Research and Development Program 2006CB200304 and 2006CB705800" and "the National Natural Science Foundation of China under Grant number 20606015 and 90410017" for funds.

Appendix A. The interrelation between collection efficiency and collection kernel

The grade number collection efficiency, $\eta_n(d_p, x)$, is a key performance parameter of ESPs, which is defined as the ratio of the number of the collected particles of d_p at x to the initial number of particles of d_p:

$$\eta_n(d_p,x) = 1 - \frac{N_p(d_p,x)}{N_p(d_p,0)} = 1 - \frac{\int_{d_p^-}^{d_p^+} n_p(d_p,x)\mathrm{d}d_p}{N_p(d_p,0)}, \qquad \text{(A-1)}$$

where d_p^- and d_p^+ denote the lower and upper limit of the section of diameter d_p, respectively.

The two sides of Eq. (1) are integrated by variable d_p from d_p^- to d_p^+, and then the following equation is obtained

$$\frac{dN_p(d_p,x)}{\mathrm{d}x} = -R(\mathrm{d}_p,x)N_p(d_p,x), \qquad \text{(A-2)}$$

So, $N_p(d_p,x) = N_p(d_p,0)\ \exp\ [-R(d_p,x)x]$. According to Eq. (A-1), the collection kernel is related with the grade number efficiency by the following equation:

$$\eta_n(d_p,x) = 1 - \exp[-R(d_p,x)x]. \qquad \text{(A-3)}$$

The grade mass collection efficiency, which is defined as the ratio of the total mass of the collected particles of d_p at x to the initial total mass of particles of d_p, is as follows:

$$\eta_m(d_p,x) = 1 - \frac{M_p(d_p,x)}{M_p(d_p,0)} = 1 - \frac{\int_{d_p^-}^{d_p^+} \rho_p \pi \frac{d_p^3}{6} n_p(d_p,x)\mathrm{d}d_p}{\int_{d_p^-}^{d_p^+} \rho_p \pi \frac{d_p^3}{6} n_p(d_p,0)\mathrm{d}d_p} \approx \eta_n(d_p,x). \qquad \text{(A-4)}$$

The overall mass efficiency, $\eta_{om}(x)$, is the ratio of the total mass of the collected particles over all particle size at x to the initial total mass of particles:

$$\eta_{om}(x) = 1 - \frac{\int_0^\infty \rho_p \pi \frac{d_p^3}{6} n_p(d_p,x)\mathrm{d}d_p}{\int_0^\infty \rho_p \pi \frac{d_p^3}{6} n_p(d_p,0)\mathrm{d}d_p} = \frac{\int_0^\infty \eta_m(d_p,x) d_p^3 n_p(d_p,0)\mathrm{d}d_p}{\int_0^\infty d_p^3 n_p(d_p,0)\mathrm{d}d_p}. \qquad \text{(A-5)}$$

The overall number efficiency, $\eta_{on}(x)$, is calculated by:

$$\eta_{on}(x) = 1 - \frac{\int_0^\infty n_p(d_p,x)\mathrm{d}d_p}{\int_0^\infty n_p(d_p,0)\mathrm{d}d_p} = \frac{\int_0^\infty \eta_n(d_p,x) n_p(d_p,0)\mathrm{d}d_p}{\int_0^\infty n_p(d_p,0)\mathrm{d}d_p}. \qquad \text{(A-6)}$$

$N_p(x)$, the geometric mean volume $v_{pg}(x)$, $d_{pg}(x)$, $\sigma_{pg}(x)$, $\eta_{on}(x)$, $\eta_{om}(x)$, $\eta_n(x)$, $\eta_m(x)$, and $Y(d_p, x)$ are computed in the MC method as follows, respectively:

$$N_p(x) = \int_{d_{p,\min}}^{d_{p,\max}} n_p(d_p,x)\mathrm{d}d_p = \sum_{i=1}^{N_{pf}} w_{pi}; \qquad \text{(A-7)}$$

$$v_{pg}(x) = \exp\left(\sum_{i=1}^{N_{pf}} w_{pi}\ln(v_{pi}) \Big/ \sum_{i=1}^{N_{pf}} w_{pi}\right)$$

$$d_{pg}(x) = [6v_{pg}(x)/\pi]^{1/3}; \qquad \text{(A-8)}$$

$$\sigma_{pg}(x) = \exp\left\{\sqrt{\sum_{i=1}^{N_{pf}} w_{pi}\ln^2[v_{pi}/v_{pg}(x)] \Big/ \sum_{i=1}^{N_{pf}} w_{pi}}\right\}; \qquad \text{(A-9)}$$

$$\eta_{om}(x) = 1 - \frac{\int_0^\infty \rho_p \pi \frac{d_p^3}{6} n_p(d_p,x)\mathrm{d}d_p}{\int_0^\infty \rho_p \pi \frac{d_p^3}{6} n_p(d_p,0)\mathrm{d}d_p} = 1 - \frac{\sum_{i=1}^{N_{pf}} d_{pi}^3 w_{pi}}{\sum_{i=1}^{N_{pf}} d_{pi}^3 w_{pi}(0)}; \qquad \text{(A-10)}$$

$$\eta_{on}(x) = 1 - \frac{\int_0^\infty n_p(d_p,x)\mathrm{d}d_p}{\int_0^\infty n_p(d_p,0)\mathrm{d}d_p} = 1 - \frac{\sum_{i=1}^{N_{pf}} w_{pi}}{\sum_{i=1}^{N_{pf}} w_{pi}(0)}; \qquad \text{(A-11)}$$

$$\eta_n(d_p,x) \approx \eta_m(d_p,x) = 1 - \int_{d_p^-}^{d_p^+} n_p(d_p,x)\mathrm{d}d_p / N_p(d_p,0)$$
$$= 1 - \sum_{i=1}^{N_{pf}} w_{pi}\delta(d_{pi},d_p) / \sum_{i=1}^{N_{pf}} w_{pi}(0); \quad \text{(A-12)}$$

$$Y(d_p,x) = \int_0^{d_p} \rho_p \pi \frac{d_p^3}{6} n_p(d_p,x)\mathrm{d}d_p / \int_0^{\infty} \rho_p \pi \frac{d_p^3}{6} n_p(d_p,x)\mathrm{d}d_p$$
$$= 1 - \sum_{i=1}^{N_{pf}} d_{pi}^3 w_{pi}\theta(d_{pi} > d_p) / \sum_{i=1}^{N_{pf}} d_{pi}^3 w_{pi}. \quad \text{(A-13)}$$

where $w_{pi}(0)$ is the initial number weight of fictitious particle i in the EDCV method. $\delta(d_{pi}, d_p)$ is Dirac delta function, $\delta(d_{pi}, d_p) = 1$ only if $d_p = d_{pi}$, otherwise $\delta(d_{pi}, d_p) = 0$; $\theta(X)$ is a conditional function, when the condition X is satisfied, $\theta(X) = 1$, otherwise $\theta(X) = 0$.

References

[1] Liu JZ, Fan HY, Zhou JH, Cao XY, Cen KF. Experimental studies on the emission of PM_{10} and $PM_{2.5}$ from coal–fired boiler. Proc CSEE 2003;23:145–9.

[2] Deutsch W. Bewegung und Ladung der Elektrizitatstrager im Zylinderkondensator. Ann Phys 1922;68:335–44.

[3] Cooperman G. A unified efficiency theory for electrostatic precipitators. J Atmos Environ 1984;18:277–85.

[4] Leonard GL, Mitchner M, Self SA. Particle transport in electrostatic precipitators. J Atmos Environ 1980;14:1289–99.

[5] Zhao ZB, Zhang GQ. New model of electrostatic precipitation efficiency accounting for turbulent mixing. J Aerosol Sci 1992;23:115–21.

[6] Zhang XR, Wang LZ, Zhu KQ. An analysis of a wire-plate electrostatic precipitator. J Aerosol Sci 2002;33:1595–600.

[7] Nóbrega SW, Falaguasta MCR, Coury JR. A Study of a wire-plate electrostatic precipitator operating in the removal of polydispersed particles. Braz J Chem Eng 2004;21:275–84.

[8] Soldati A, Andreussi P, Banerjee S. Direct simulation of turbulent particle transport in electrostatic precipitators. AIChE J 1993;39:1910–9.

[9] Soldati A, Casal M, Andreussi P, Banerjee S. Lagrangian simulation of turbulent particle dispersion in electrostatic precipitators. AIChE J 1997;43:1403–13.

[10] Soldati A. On the effects of electrohydrodynamic flows and turbulence aerosol transport and collection in wire-plate electrostatic precipitators. J Aerosol Sci 2000;31:293–305.

[11] Gallimberti I. Recent advancements in the physical modelling of electrostatic precipitators. J Electrostat 1998;43:219–47.

[12] Choi BS, Fletcher CAJ. Turbulent particle dispersion in an electrostatic precipitator. Appl Mathemat Model 1998;22:1009–21.

[13] Park SJ, Kim SS. Effects of particle space charge and turbulent diffusion on performance of plate–plate electrostatic precipitators. J Electrostat 1998;45:121–37.

[14] Park JH, Chun CH. An improved modelling for prediction of grade efficiency of electrostatic precipitators with negative corona. J Aerosol Sci 2002;33:673–94.

[15] Bai H, Lu C, Chang CL. A model to predict the system performance of an electrostatic precipitator for collecting polydisperse particles. J Air Waste Manage Assoc 1995;45:908–16.

[16] Kim SH, Park HS, Lee KW. Theoretical model of electrostatic precipitator performance for collecting polydisperse particle. J Electrostat 2001;50:177–90.

[17] Kallio GA, Stock DE. Interaction of electrostatic and fluid dynamic fields in wire-plate electrostatic precipitators. J Fluid Mech 1992;240:133–66.

[18] Leonard GL, Mitchner M, Self SA. An experimental study of the electrohydrodynamic flow in electrostatic precipitators. J Fluid Mech 1983;127:123–40.

[19] Kim SH, Lee KW. Experimental study of electrostatic precipitator performance and comparison with existing theoretical prediction models. J Electrostat 1999;48:3–25.

[20] Blanchard D, Dumitran LM, Atten P. Effect of electro-aero-dynamically induced secondary flow on transport of fine particles in an electrostatic precipitator. J Electrostat 2001;51–52:212–7.

[21] Salcedo R, Munz RJ. The effect of particle shape on the collection efficiency of laboratory-scale precipitators. In: Proceedings of the third international conference on electrostatic precipitation, Abano-Padova, Italy, 1987. p. 343–59.

[22] Cochet R. Lois charge des fines particules (Submicroniques) Etudes théoriques – Controles récents spectre de particules, Colloque International la Physique des Forces Electrostatiques et Leurs Application. Centre National de la Recherche Scientifique, Paris, France, 1961. p. 331–8.

[23] Yoo KH, Lee JS, Oh MD. Charging and collection of submicron particles in two-stage parallel plate electrostatic precipitators. Aerosol Sci Tech 1997;27:308–23.

[24] Zhao HB, Zheng CG. A stochastic algorithm for the dynamic evolution process by particle deposition. Acta Aerodynam Sinica 2006;24:141–6.

[25] Zhao H, Zheng C. Monte Carlo solution of wet removal of aerosols by precipitation. Atmos Environ 2006;40:1510–25.

[26] Zhao H, Maisels A, Matsoukas T, Zheng C. Analysis of four popular Monte Carlo methods for solution of population balances in dispersed systems. Powder Technol 2007;173:38–50.

[27] Zhao H, Zheng C, Xu M. Multi-Monte Carlo method for coagulation and condensation/evaporation in dispersed systems. J Colloid Interf Sci 2005;286:195–208.

[28] Garcia AL, van den Broek C, Aertsens M, Serneels R. A Monte Carlo simulation of coagulation. Physica 1987;143A:535–46.

[29] Maisels A, Kruis FE, Fissan H. Direct simulation Monte Carlo for simultaneous nucleation, coagulation, and surface growth in dispersed systems. Chem Eng Sci 2004;59:2231–9.